NOLTR 69-215

A THEORETICAL AND EXPERIMENTAL INVESTIGATION OF SNAP LOADS IN STRANDED STEEL CABLES

By
Jack E. Goeller

26 NOVEMBER 1969

NOL
UNITED STATES NAVAL ORDNANCE LABORATORY, WHITE OAK, MARYLAND

NOLTR 69-215

38

A THEORETICAL AND EXPERIMENTAL INVESTIGATION OF SNAP LOADS IN STRANDED STEEL CABLES

Prepared by:
Jack E. Goeller

ABSTRACT: One of the problems encountered in supporting payloads by a cable system exposed to longitudinal excitation simulating ocean wave motion is referred to as cable snap. This is due to a combination of wave amplitude and frequency which causes slack in the cable during upward movement of the payload. During descent of the payload, the cable becomes taut and a severe impact load is experienced. This phenomenon was modeled on an analog computer assuming elastic cables, and by a digital computer program assuming segmented cables of two viscoelastic materials. These mathematical models were shown to give good agreement with experiments on 1/16-inch and 3/32-inch stranded steel cables of length up to 70 feet with a 27-pound spherical payload attached to the lower end. Snap forces as high as nine times the static force from the payload were encountered. It was shown that these snap forces can be significantly mitigated by the addition of a short length of nylon rope added to the bottom of the cable. It then is possible to get through the snap condition by increasing the frequency in much the same way that it is possible to get through a resonant condition.

U. S. NAVAL ORDNANCE LABORATORY
WHITE OAK, MARYLAND

NOLTR 69-215 26 November 1969

A THEORETICAL AND EXPERIMENTAL INVESTIGATION OF SNAP LOADS IN STRANDED STEEL CABLES

This effort was conducted by the Ballistics Department for future application to buoy or moored systems. The author wishes to acknowledge the support given by Dr. P. A. Laura of the Catholic University of America and Drs. A. E. Seigel, V. C. D. Dawson, and J. C. S. Yang of the Naval Ordnance Laboratory.

GEORGE G. BALL
Captain, USN
Commander

A. E. Seigel

A. E. SEIGEL
By direction

CONTENTS

ILLUSTRATIONS

ILLUSTRATIONS (Cont.)

TABLES

REFERENCES

1. Schneider, L., Mahand, T., and Burton, L., "Tow Cable Snap Loads," ASME Paper 64-WA/UNT-8, Dec 1964
2. Richardson, William S., "Buoy Mooring Cables, Past, Present and Future," Transactions, 2nd International Buoy Technology Symposium, 18 Sep 1967
3. Goeller, J. E., "A Theoretical and Experimental Investigation of a Flexible Cable System Subjected to Longitudinal Excitation," Ph.D. Dissertation, Catholic University, 1969
4. Snyder, A. E., Jerabek, J. C., and Whitney, C., "Constant-Tension Oceanographic Winch," ASME Paper 63-WA-335, Oct 1963

LIST OF SYMBOLS

A_p projected cross-sectional area of spherical payload $A_p = .785\ D^2$

A_c wetted area of cable $A_c = \pi\ d\ L$

C damping coefficient

C_{CR} critical damping ratio $C_{CR} = 2\sqrt{k_e M_e}$

C_{DP} drag coefficient of payload

C_{DC} drag coefficient of cable

D diameter of payload mass

d diameter of cable

E modulus of elasticity

F_s preload in foundation spring

g gravitation constant

k spring constant

k_e effective spring constant of segmented cable $\frac{1}{k_e} = \frac{1}{k_3} + \frac{1}{k_2}$

L length of cable

ℓ length of drive rod

M_C effective mass of cable

M_e effective mass $= M_p + M_{vm}$

M_p mass of payload

M_{vm} virtual mass of displaced water

P axial force in cable

p perimeter of cable

W_B buoyancy force due to displaced payload

LIST OF SYMBOLS (Cont.)

W_P	weight of payload
x	spatial variable
x_o	maximum amplitude of displacement function
δ_{sp}	static deflection of payload
δ_{sc}	static deflection of lumped cable mass
τ	time constant of viscoelastic model
ω_{ne}	natural frequency of simple spring mass system; $$\omega_{ne} = \sqrt{\frac{k_e}{M_e}}$$
ω	circular frequency of forcing function

SUBSCRIPTS

p	payload
c	cable
e	effective
s	external spring
1, 2, 3	applies to segments of cable (see Figs. 1 and 4)

INTRODUCTION

Cable systems using stranded wire rope are frequently used in a number of commercial and military applications. In salvage and towing operations, for example, large objects are suspended from a ship which is exposed to ocean wave motion. The approximate sinusoidal motion of the waves can cause dynamic stresses in the cable which are significantly higher than the static force from the payload weight.

One of the problems in supporting large payloads by a cable which is excited sinusoidally at the upper end is often referred to as cable snap (Ref. 1). The net cable force is composed of the static tensile force due to the payload weight (minus buoyancy force) and the dynamic force which is either compressive or tensile. When the compressive component exceeds the static tensile force, the cable goes slack. The cable is subsequently subjected to severe impact stresses when it again becomes taut. Impending slack occurs when the net cable force reaches zero.

This phenomenon of snap loading was studied on small-scale models in laboratory experiments. The purpose of this report is to develop mathematical models to predict the phenomenon observed. In order to have generality, a segmented cable system of nylon and steel was considered. Nylon is frequently used because of its light weight and ease of handling. It will be shown in this report that it has the added feature of being a good material for mitigating snap loads. Conventional steel stranded cable is considered since it is frequently used in salvage operations, and, moreover, it is generally used in the upper portion of most deep ocean cable systems to prevent fish bite (Ref. 2).

MATHEMATICAL MODELS

Two models were used to compute the cable force before and during snap conditions. The first model, which is similar to that of reference 1, is the simplest in that it is a single-degree-of-freedom system with nonlinear payload damping. The model applies only to elastic cables. The second model is more general in that it applies to a segmented cable of two viscoelastic materials and considers nonlinear damping of both the cable and the payload. A distributed mass model (Ref. 3) was investigated by the author and it was found that the lumped parameter models yield a good approximation to the distributed mass model over the fundamental frequency range, provided slack does not occur in the cable and the mass of the cable is small compared to the mass of the payload.

a. Model No. 1: Analog Simulation

The first model consists of a simple single-degree-of-freedom system as shown in Figure 1. The dynamic equation of motion with respect to the equilibrium position is

$$M_e \ddot{x}_2 + \frac{1}{2} \rho \quad C_{DP} A_P \left| \dot{x}_2 \right| \dot{x}_2 + K_c (x_2 - x_1) = 0 \qquad (1)$$

The total force in the cable is that due to the dynamic force $K_C (x_2 - x_1)$ and that due to static force $T_{STAT} = W_P - W_B$.

The inertia force $M_e \ddot{x}_2$ includes the mass of the payload which is considered to be a sphere and the virtual mass of water. An effective cable mass of one-third the actual mass was lumped with the payload mass. The virtual mass of the cable is negligible.

The drag force is considered to be proportional to the square of the payload velocity. The drag coefficient is taken as constant at 0.50. The basis for this selection can be seen from Figure 22 of reference 2, showing the drag coefficient for a sphere versus Reynolds number. The drag coefficient is fairly constant over a range of Reynolds numbers of 500 to 3 x 10^5. For the experiments conducted, the Reynolds number was well within this range. Absolute value on velocity is used so that the drag force is always opposite to the direction of motion for both positive and negative x_2.

The spring force is based on the spring constant of the cable and the supporting structure. For the experiments performed, the spring constant of the cable was very much greater than that of the support structure. Hence

$$K_C = \frac{AE}{L}$$

The static force T_{STAT} is simply the dry payload weight minus the buoyancy force of the displaced fluid.

For purposes of solution on the analog computer, it is convenient to rewrite equation (1) as

$$\ddot{x}_2 = - \frac{1}{2} \frac{\rho \, C_{DP} \, A_P}{M_e} \left| \dot{x}_2 \right| \dot{x}_2 - \frac{K_C}{M_e} (x_2 - x_1) \qquad (2)$$

The forcing function for simulation of an ocean wave is generally taken as sinusoidal. In the experiments performed, a bell crank device was used as shown in Figure 2, which generates a forcing function which is not completely sinusoidal. For a constant rotational speed ω, the forcing function x_p can be shown to be

$$x_p = x_o \sin \omega t + \frac{x_o^2}{4\ell} (\cos 2 \omega t - 1) \tag{3}$$

The function is very nearly sinusoidal when $\frac{x_o}{4\ell}$ is made very small compared to 1.0 where x_o is the amplitude of the wave (radius of flywheel) and ℓ is the length of the driving rod. For the experiments performed, $\frac{x_o}{4\ell}$ has a maximum value of 0.019, which is as small as it could be practically made. This results in a very small deviation from purely sinusoidal input. Computations using a purely sinusoidal function were compared to those using equation (3), and little difference was observed.

Equation (2) is valid provided the total cable force given by

$$F_C = W_P - W_B + K_C (x_2 - x_1) \tag{4}$$

is greater than, or equal to, zero. When this force attempts to go compressive (negative), it must be set equal to zero since the cable cannot support a compressive force. The cable then goes slack so that during the slack regime the equation of motion is

$$\ddot{x}_2 = - \frac{1}{2} \frac{\rho C_{DP} A_P}{M_e} \left| \dot{x}_2 \right| \dot{x}_2 - \frac{W_P - W_B}{M_e} \tag{5}$$

This is the equation of motion of a body in free flight given an initial acceleration. It eventually reaches a peak, then it descends until the cable becomes taut, at which time it again feels the spring force. Equation (2) then applies again with the initial conditions the same as the final conditions of the slack regime.

The previous equations were solved on the analog computer. The setup is shown in Figure (3). The setup incorporates a limiting diode which discriminates the cable force to insure it is positive or zero. Negative values (compression) are set equal to zero and equation (5) is solved.

b. <u>Model No. 2: Digital Program Solution</u>

The details of the model are illustrated in Figure 4. The viscoelastic behavior of each cable segment is approximated by a Voigt model. The cable mass is considered as a lumped parameter along with the cable damping. The drag force on the cable and payload is considered to be proportional to the velocity squared with a constant drag coefficient. The payload mass is considered to be held to a rigid foundation by an elastic spring and dashpot to simulate an object held by the ocean sediments. These were included to solve other problems such as breakaway of an object held by the ocean sediments. A constant static force "F_S" is added to simulate a lifting force during a salvage operation. For free oscillation, $K_S = F_S = C_S = 0$. In order to incorporate a snap criteria, it is convenient to express the dynamic equations of motion with respect to a coordinate system relative to the end of the cable in an unstressed configuration. The equation of motion of the payload then becomes

$$M_e \ddot{x}_2 + \frac{1}{2} \rho C_{DP} A_P \left|\dot{x}_2\right| \dot{x}_2 + K_2 (x_2 - x_3) + C_2 (\dot{x}_2 - \dot{x}_3) +$$

$$K_s x_2 + C_s \dot{x}_2 - (W_P - W_B) - F_s = 0 \tag{6}$$

The force in segment 2 of the cable is

$$P_2 = K_2 (x_2 - x_3) + C_2 (\dot{x}_2 - \dot{x}_3) \tag{7}$$

The equation of motion of the lumped cable mass is

$$M_c \ddot{x}_3 + \frac{1}{2} \rho C_{DC} A_C \left|\dot{x}_3\right| \dot{x}_3 + K_3 (x_3 - x_1) + C_3 (\dot{x}_3 - \dot{x}_1) -$$

$$K_2 (x_2 - x_3) - C_2 (\dot{x}_2 - \dot{x}_3) - (W_C - W_{CB}) = 0 \tag{8}$$

The force in segment 3 of the cable is

$$P_3 = K_3 (x_3 - x_1) + C_3 (\dot{x}_3 - \dot{x}_1) \tag{9}$$

The forcing function is again taken in the form

$$x_1 = - \left[x_o \sin \omega t + \frac{x_o^2}{4\ell} (\cos 2 \omega t - 1) \right] \tag{10}$$

The initial boundary conditions at time equal to zero are that the initial velocities $\dot{x}_2$ (0) and $\dot{x}_3$ (0) be equal to zero. Since the coordinate system is relative to an unstressed cable, the initial displacements of x_2 and x_3 must be computed. This can be done from equations (6) and (7) for velocities and accelerations equal to zero. Hence, for the payload and lumped mass, we obtain:

$$\delta_{sP} = x_2\ (0) = \frac{F_s + W_P - W_B + \frac{K_2}{K_2 + K_3}(W_C - W_{CB})}{K_2 + K_s - \frac{K_2^{\ 2}}{K_2 + K_3}} \tag{11}$$

$$\delta_{sc} = x_3\ (0) = \frac{W_C - W_{CB} + K_2\ x_2\ (0)}{K_2 + K_3} \tag{12}$$

The equations developed were programmed on the digital computer. However, the equations must be modified in the regime of slack which subsequently causes the snap loads.

There are three possible conditions for snap in the cable as modeled. They are as follows:

(1) The bottom cable segment goes slack ($P_2 = 0$)

(2) The top cable segment goes slack ($P_3 = 0$)

(3) Both the top and bottom segments go slack ($P_2 = P_3 = 0$)

The equations of motion for each of these conditions during the time period of slack can be obtained by setting the appropriate cable force equal to zero. In effect, the cable force in each segment must always be positive or zero, but never negative, since the cable cannot support a compressive load (note that in the convention used, tension is positive).

Now consider condition one where only the bottom segment goes slack. The appropriate equations in the non-slack time regime are:

$$\ddot{x}_2 = -\frac{1}{2}\frac{\rho\ C_{DP}\ A_P}{M_e}\left|\dot{x}_2\right|\ \dot{x}_2 - \frac{K_2}{M_e}(x_2 - x_3) - \frac{C_2}{M_e}(\dot{x}_2 - \dot{x}_3) +$$

$$\frac{W_P - W_B}{M_e} + \frac{F_s}{M_e} - \frac{K_s\ x_2}{M_e} - \frac{C_s\ \dot{x}_2}{M_e} \tag{13}$$

$$\ddot{x}_3 = -\frac{1}{2}\frac{\rho\ C_{DC}\ A_C}{M_C}\left|\dot{x}_3\right|\ \dot{x}_3 - \frac{K_3}{M_C}(x_3 - x_1) - \frac{C_3}{M_C}(\dot{x}_3 - \dot{x}_1) +$$

$$\frac{K_2}{M_C}(x_2 - x_3) + \frac{C_2}{M_C}(\dot{x}_2 - \dot{x}_3) + \frac{W_C - W_{CB}}{M_C} \tag{14}$$

Impending slack occurs when P_2 tries to go negative while P_3 is still positive, viz

$$P_2 = K_2\ (x_2 - x_3) + C_2\ (\dot{x}_2 - \dot{x}_3) \le 0$$

$$P_3 = K_3\ (x_3 - x_1) + C_3\ (\dot{x}_3 - \dot{x}_1) \ge 0$$

Then during the slack regime $P_2 = 0$. Hence

$$\ddot{x}_2 = -\frac{1}{2}\frac{\rho\ C_{DP}\ A_P}{M_e}\left|\dot{x}_2\right|\ \dot{x}_2 + \frac{W_P - W_B}{M_e} + \frac{F_s}{M_e} - \frac{K_s}{M_e}\ x_2 - \frac{C_s}{M_e}\ \dot{x}_2$$

$$\ddot{x}_3 = -\frac{1}{2}\frac{\rho\ C_{DC}\ A_C}{M_C}\left|\dot{x}_3\right|\ \dot{x}_3 - \frac{K_3}{M_C}\ (x_3 - x_1) - \frac{C_3}{M_C}\ (\dot{x}_3 - \dot{x}_1) + \frac{W_C - W_{CB}}{M_C} \tag{15}$$

Now consider condition two where only the top segment goes slack. Equations (13) and (14) still apply in the non-slack regime. For slack to initiate in the top segment only, it is necessary that:

$$P_2 = K_2\ (x_2 - x_3) + C_2\ (\dot{x}_2 - \dot{x}_3) \ge 0$$

$$P_3 = K_3\ (x_3 - x_1) + C_3\ (\dot{x}_3 - \dot{x}_1) \le 0$$

Then in the slack time regime $\ddot{x}_2$ is still given by equation (13) while P_3 is set equal to zero in equation (14), yielding the following:

$$\ddot{x}_3 = -\frac{1}{2}\frac{\rho\ C_{DC}\ A_C}{M_C}\left|\dot{x}_3\right|\ \dot{x}_3 + \frac{K_2}{M_C}\ (x_2 - x_3) + \frac{C_2}{M_C}\ (\dot{x}_2 - \dot{x}_3) + \frac{W_C - W_{CB}}{M_C} \tag{16}$$

For impending slack in both top and bottom segments, the equations of motion for the slack regime are obtained by setting both P_2 and P_3 equal to zero. Hence, in the slack regime we obtain:

$$\ddot{x}_2 = -\frac{1}{2}\frac{\rho C_{DP} A_P}{M_e}\left|\dot{x}_2\right|\dot{x}_2 + \frac{W_P - W_B}{M_e} + \frac{F_s}{M_e} - \frac{K_s}{M_e}x_2 - \frac{C_s}{M_e}\dot{x}_2 \qquad (17)$$

$$\ddot{x}_3 = -\frac{1}{2}\frac{\rho C_{DC} A_C}{M_C}\left|\dot{x}_3\right|\dot{x}_3 + \frac{W_C - W_{CB}}{M_C} \qquad (18)$$

The previous equations were programmed on the 7090 computer. Basically, the program computes the cable forces and displacements from the differential equations (equations (13) and (14)), which are initialized according to the boundary conditions of displacement and velocity. Then forces in the cable are computed and checked to determine if the force in either cable segment is negative. If either or both forces are negative, the program switches to applicable equations which have no cable force, viz, the slack regime. It then computes the displacement according to these equations for the following time steps until the cable force becomes positive, at which time it switches back to the original equations. The program is written to permit the frequency to be put in as a step function, ramp function, or a combination of ramps and steps as illustrated below. Printout is given for both transient and steady-state phases.

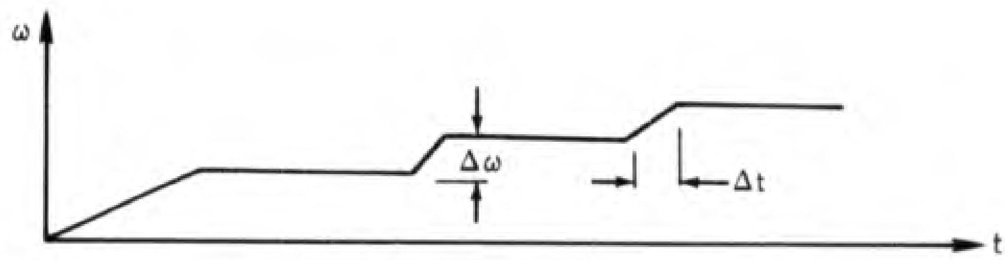

TEST APPARATUS

The tests were performed at the Naval Ordnance Laboratory using the Hydroballistics Tank shown in Figure 5. The tank is approximately 35 feet wide by 100 feet long with a water level of up to 65 feet. The water is of high purity. The driving mechanism for oscillating the cable was located on the top deck with the cable inserted through a porthole in the deck. A portion of the cable length was in air while the major portion was immersed in the water. The payload could be photographed through ports in the sides of the tank.

The driving mechanism for oscillating the cable is shown in Figure 6. It is essentially a crank-type device with a drive rod attached to the flywheel. The prime mover consisted of a d-c shunt electric motor with a reduction gear for reducing the speed and increasing the torque capability. The motor had adjustable speed, but at a given setting the speed was insensitive to changes in the applied torque.

The force in the cable specimens was measured by load cells located at top and bottom of the cable. The load cell used was Model A 8293 as manufactured by Schaevitz with a maximum load capability of 1000 pounds. The voltage output was fed to a Beckman-type R oscillograph where a trace of force versus time was obtained. Prior to each test, the instrument was calibrated by applying known weights to the load cells. In tests involving short rise times during impact, a Honeywell Visicorder oscillograph was used with a frequency response of 50 kc.

TEST SPECIMENS

Two basic types of cables were studied; namely, steel and segmented cables of steel and nylon braided rope. The steel cables can best be described as "aircraft type." This type was used because of its availability in small sizes. The diameters of cable studied were 1/16 inch and 3/32 inch. All cables were carbon steel to MIL-W-1511 with a galvanized coating and consisted of seven wires per strand with seven strands per cable (7 x 7). Male-type fittings were swaged on each end of the cable. A listing of pertinent characteristics of the specimens is shown in Table 1. Experimental force versus extension on full-length cables was obtained to determine the spring constant. The unloading phase exhibited some hysteresis. After the cable was loaded to about 10 pounds, the force-extension curve was fairly linear. The results compared reasonably well with those published by the cable supplier.

The payload was a sphere of 8-inch diameter which was made of solid aluminum with a weight of 26.9 pounds, including attachment fittings. Aluminum was used to get a relatively high payload density (173 lbs/ft^3). A high payload density was desired to delay the snap loading condition to as high a frequency ratio ω/ω_{ne} as possible. A high density payload yields a high initial static stress and low natural frequency. Both effects delay the snap condition. Steel spheres were considered, but the payload density is beyond practicality. The weight of the sphere in water is 17.3 pounds, excluding the weight of the attached cable. The virtual mass or added mass of displaced water is 0.15 slugs (4.85 pounds).

TEST RESULTS

Forced oscillation tests were conducted on both 1/16-inch and 3/32-inch stranded cables of 62-foot and 70-foot length. The forcing frequency was increased in small steps and held until steady-state conditions were achieved. Typical force versus time responses are shown in Figure 7 for a 1/16-inch cable 62 feet long oscillated at various frequencies. At low frequency the force response is approximately sinusoidal. However, as the frequency was increased, nonlinearities were encountered as evidenced by the double peak. This behavior was very reproducible and is believed to be caused primarily by the nonlinear water damping. This same type response was observed in the analog using mathematical model No. 1 previously discussed. The forcing frequency was increased until snap occurred at about 1.27 Hz as shown in Figure 7d. There was a drastic increase of force in the cable peaking to about 130 pounds. After two minutes or 100 cycles, the cable fitting attached to the mass fractured. The recorded force at the time of failure was about 150 pounds. The rated strength of the cable is 475 pounds. The rated strength of the swaged-on cable fitting is 90 percent of the cable strength, or 410 pounds. A failure analysis indicated that the most probable cause of the premature failure was a combined bending stress and axial stress caused by angular orientation of the payload when snap occurred. Photographic coverage indicated a tendency for the payload to tilt off the vertical during free flight (slack condition). Hence, when snap initiated, a bending stress was induced in the cable fitting since the fitting is essentially clamped in one direction. This bending stress can be significantly alleviated by a swivel-type joint.

Tests were also performed in water on 1/16-inch and 3/32-inch cables of 70 feet in length. The excitation amplitudes were two and three inches. The additional length of cable resulted in a lower spring constant and, hence, slightly lower snap force. In general, it was found that the snap load is less severe as the cable flexibility increases. The shape of force pulses for these tests was very similar to those previously described for the shorter cables.

Figure 9 shows the theoretical results from the analog run (Model No. (1)) for the displacement amplitude x_1, the payload amplitude x_2, and the force in the cable during a snap condition. From point A to point B, the cable is slack. From point B to C, the cable experiences the snap load. These particular curves are for a frequency of 1.25 Hz. The computed snap load is 155 pounds. If one compares this with Figure 7 of the test data, the experimental snap load at the top of the cable is about 150 pounds.

The maximum experimental cable force as a function of forcing frequency was compared with theory for the 1/16-inch-diameter cable and the 3/32-inch-diameter cable. Both the analog model (No. 1) and digital program model (No. 2) were used. It was found that both give about the same results for steel cables which exhibit elastic behavior provided the mass of the cable is small compared to the mass of the payload, and the payload damping is large compared to the cable damping.

Figure 9 shows the experimental maximum cable force in 1/16-inch cable compared to predictions from model No. 1 and model No. 2. In the low-frequency range the comparison is quite good. The snap load occurred at about the predicted forcing frequency. The theory predicts successive peaks in snap load. The first peak was predicted to be 155 pounds at about 1.28 Hz. The maximum force experienced in the test was about 150 pounds. This is close to the first peak. Unfortunately, the cable and fitting broke before higher loads could be developed. It is very doubtful if the minimum value predicted by theory could have been observed in the tests on steel cables since the force is so sensitive to forcing frequency once the snap is initiated. A slight increase in frequency results in a significant increase in cable force. However, it was demonstrated later that by adding a small section of nylon rope to the 3/32-inch steel cable, the snap load could be mitigated by the added flexibility of the nylon. A peak snap load was observed which was followed by a minimum and then a rapid increase in load.

Figure 10 shows the comparison for 3/32-inch-diameter cable for displacement amplitude of 2 and 3 inches. The agreement is good in the low-frequency range. The initiation of snap occurs at a slightly lower frequency than expected. For the 2-inch displacement, the maximum force encountered was 170 pounds. Theoretically, the force should reach a peak of 300 pounds at a frequency of 1.65 Hz, then drop off slightly. Another sharp rise is then predicted. It was not possible to achieve these force levels in the experiment because of fear of damaging the apparatus. During the testing of nylon rope, it was observed that it was possible to get through the snap condition by increasing the frequency in much the same way it is possible to get through a resonance condition. The question then arose as to whether it is possible to get through the snap condition for steel cables by increasing the frequency. Certainly, the chances would be improved if a short section of nylon was added to serve as a mitigator or shock absorber. It was hoped that such a test would provide some insight as to how to design a shock absorber system for steel cables which might be expected to operate at a frequency near the critical frequency which initiates snap. The 3/32-inch-diameter steel cable previously tested was fitted with a 6-foot addition of 1/4-inch nylon at the bottom. The results then could be compared with those previously obtained for the same cable without the nylon. Typical traces of force at the top of the cable versus time for various forcing frequencies are shown in Figure 11. The displacement amplitude is 2 inches. The first snap condition occurred at a forcing frequency of 1.31 Hz and the cable force peaked to 87 pounds. The force then decreased as the frequency was increased; viz, it was possible to get through the snap condition. After getting through the snap condition, photographic coverage showed the payload to exhibit small amplitude vertical oscillation, but also exhibited a rocking motion with very little lateral movement at the center of gravity. As the frequency was increased to 2.17 Hz, violent snap loads were again encountered as shown in Figure 11d. The frequency then was decreased, and the force decreased until the first snap condition was again encountered.

Figure 12 shows the theoretical force at the top of the cable predicted by the digital program (Model No. 2) compared to the experimental results for 2-inch excitation amplitude at the top. The comparison appears to be quite good considering the complexity of the snap phenomena. It is interesting to note that the cable force does reach a maximum during the first snap condition, followed by a minimum and then a rapid increase at the second snap condition. The second snap condition occurs very near the resonant frequency of the cable system. The theory predicts the same basic type behavior with the largest error occurring in the vicinity of the minimum.

The results prove that it is possible to get through the snap condition by increasing the forcing frequency. However, a second snap condition can follow close behind. It also shows that the two-parameter lumped viscoelastic model used in the digital program (Model No. 2) yields fairly accurate results over a wide frequency range.

The test also shows that the nylon does mitigate the snap load appreciably. The same 3/32-inch steel cable was tested at 2-inch amplitude without the nylon (see Fig. 10). The snap load reached 170 pounds at 1.6 Hz and still had not yet reached the maximum. The predicted maximum for the first snap condition is 300 pounds. The same cable with the nylon addition experienced a maximum force of 90 pounds for a frequency range from 0 to 2.0 Hz.

Pertinent cable characteristics used in the digital code for the analysis are as follows:

K_2 (Nylon) = 20.4 lb/in

K_3 (Steel) = 86.4 lb/in

C_{DC} = .01 (Based on wetted area)

C_{DP} = .5

C_2 (Nylon) = $\tau K_e = .47 \dfrac{\text{lb sec}}{\text{in}}$

τ (Nylon) = .023 sec

C_2 (Steel) = 0

W_P = 26.9 lbs

W_B = 9.7 lbs

$W_{V.M.}$ = 4.85 lbs

DESIGN CONSIDERATIONS FOR MINIMIZING SNAP LOADS

Normally in designing a cable system, a high safety factor of six to eight is applied on the static wet weight of the payload. This is usually considered adequate for dynamic effects and fatigue. With this in mind, a plot was made of the ratio of maximum cable force to static force as a function of frequency ratio. This is shown in Figure 13. It is interesting to note that a force ratio of six can be easily obtained if a snap condition occurs. This condition can occur at a frequency ratio well below resonance. Hence, it is concluded that the safety factor can be purely fictitious if adequate provisions are not taken for the snap condition. The best solution is to avoid it in the cable system design. This usually means high density payloads so that the static force always exceeds the compressive part of the dynamic force. In cases where this is not possible, there are other possibilities. One is to design a compliance system (Ref. 4) which takes up the slack by a spring-actuated or pneumatic system. The goal is to obtain a constant tension by a feedback automatic control system which makes proper adjustments. A second approach is to design a shock mitigator into the cable system. This can probably be achieved by a spring-dashpot type device. The most simple mitigator which proved to work well is a short section of nylon rope. However, a more compact spring-dashpot mechanical device could be designed. A third approach can be used for payloads which operate near the ocean bottom. This involves hanging a heavy steel chain off the bottom of the payload. The chain should be long enough to lay on the ocean floor. This provides an appreciable damping effect.

CONCLUSIONS

As a result of this study, the following conclusions are made in regard to steel-stranded cables:

1. A snap condition is easily initiated in steel cables with resulting drastic increases in force. The onset of snap can be predicted by computing the frequency required to make the dynamic force plus the static force equal to zero, i.e., $T_{STAT} + P_{DYNAMIC} = 0$. The force during the snap condition can be predicted with good accuracy using the analytical models presented.

2. Once snap is initiated, the cable force rises sharply with slight increases in frequency. Theoretically, the force reaches a maximum and then decreases with increasing frequency. This was not achieved with purely steel cables, but was demonstrated by adding a small section of nylon to the cable. The maximum load during snap occurs at the top of the cable.

3. A factor of safety of six on the static cable load does not assure safe operation in a snap condition. Peak loads of nine times the static force were achieved in the tests. The magnitude of

snap force is strongly dependent on cable stiffness and excitation amplitude. The snap load appears to become more severe as the stiffness of the cable increases.

4. Snap loads can be significantly mitigated by increasing the flexibility with a soft spring-dashpot arrangement.

5. The connection of the cable to the payload is critical in surviving snap loads. Fixity caused by clamping the cable into payload fittings should be avoided because of possible bending stresses during the snap condition.

TABLE 1

CHARACTERISTICS OF CABLE TEST SPECIMENS

Spec. No.	Mat'l.	Dia.	Length	No. of Strands	Wt. 100 ft.	Dry Wt.	Spring Const. Air	Spring Const. Water	Natural Freq. Air	Natural Freq. Water	Break Str.
-	-	Inch	Ft.	-	Lbs.	Lbs.	lb/in	lb/in	Hz	Hz	Lbs.
1	St'l	3/32	62	7 x 7	1.6	.992	86.4	86.4	5.57	5.12	920
2	St'l	1/16	62	7 x 7	.75	.465	40.5	40.5	3.85	3.5	480
3	St'l	3/32	70	7 x 7	1.6	1.12	76.5	76.5	5.22	4.82	920
4	St'l	1/16	70	7 x 7	.75	.525	35.8	35.8	3.54	3.32	480
5	St'l Nylon	3/32 1/4	62 6	7 x 7 Braided	1.60 1.66	.99 .099	28	16.8	3.16	2.28	920

Natural Freq. Based on Wt. of Payload + Virtual Mass + 1/3 Cable Wt.

$26.9 + 4.85 + 1/3\ W_{cable}$

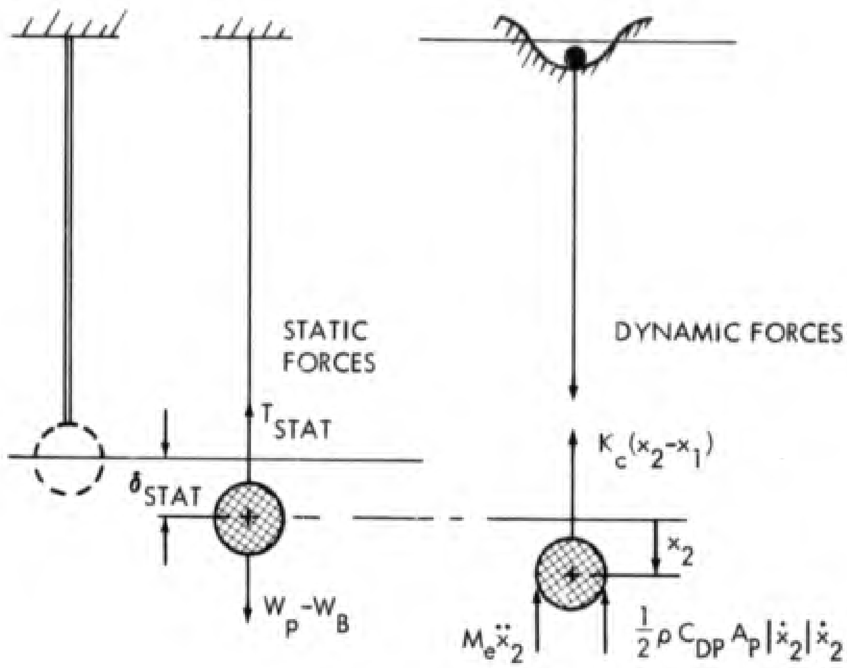

FIG. 1 STATIC AND DYNAMIC FORCES AND DISPLACEMENTS FOR ANALOG MODEL

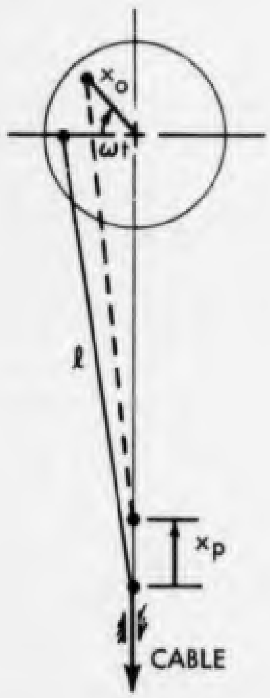

FIG. 2 ILLUSTRATION OF DRIVING MOTION APPLIED
TO TOP OF CABLE

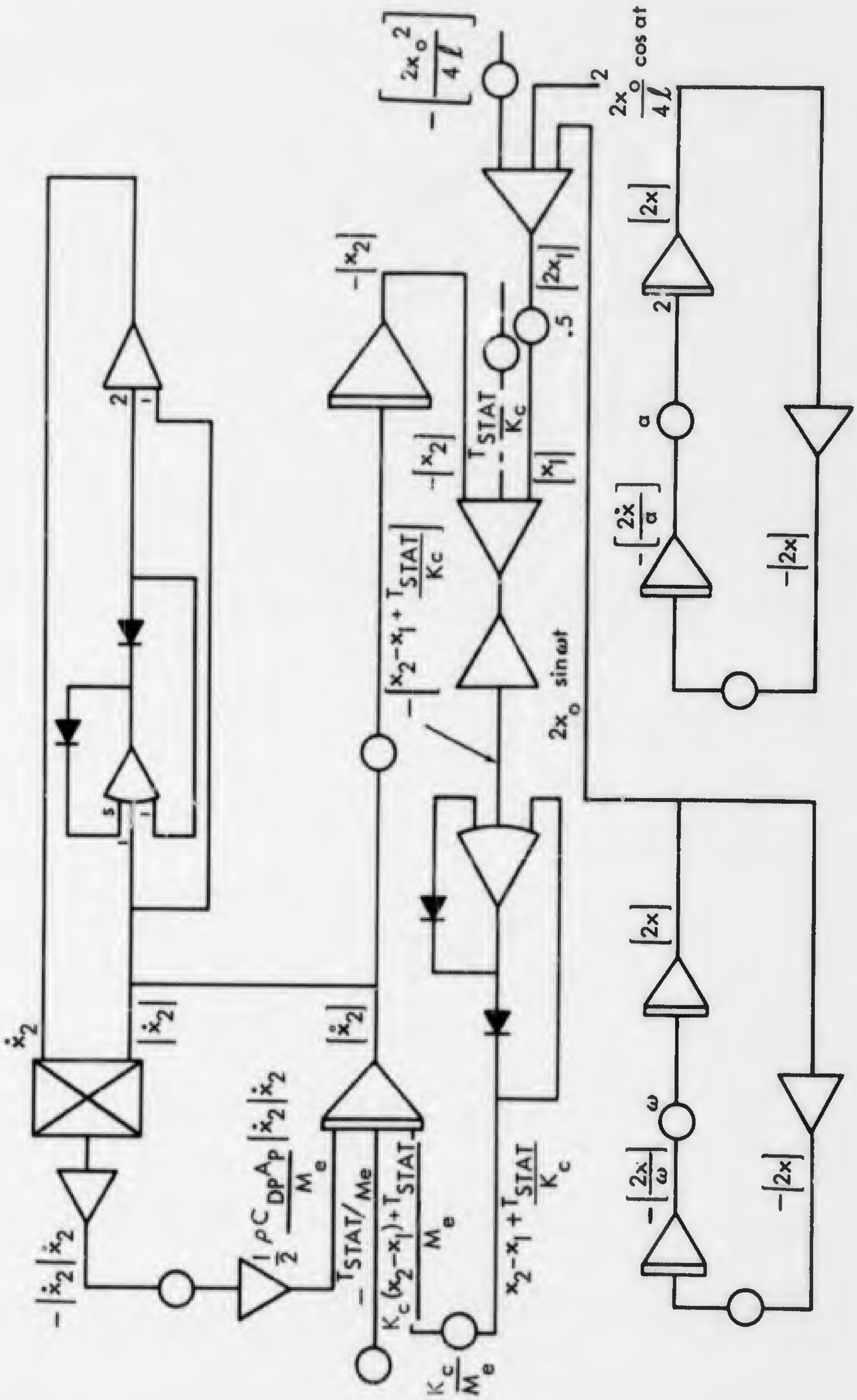

FIG. 3 ANALOG SETUP

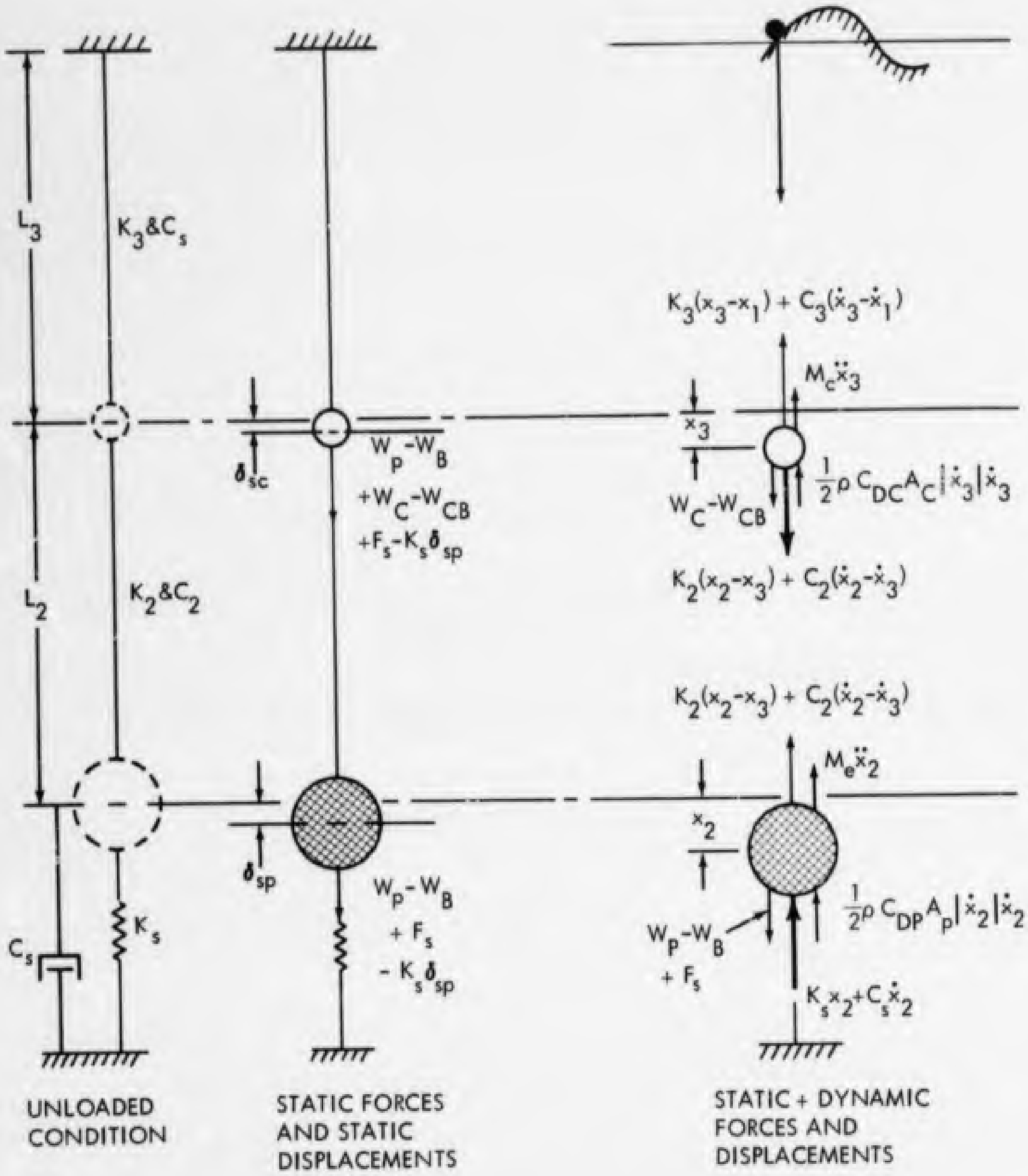

FIG. 4 ILLUSTRATION OF FORCES AND DISPLACEMENTS IN SEGMENTED CABLE SYSTEM - MODEL (NO. 2)

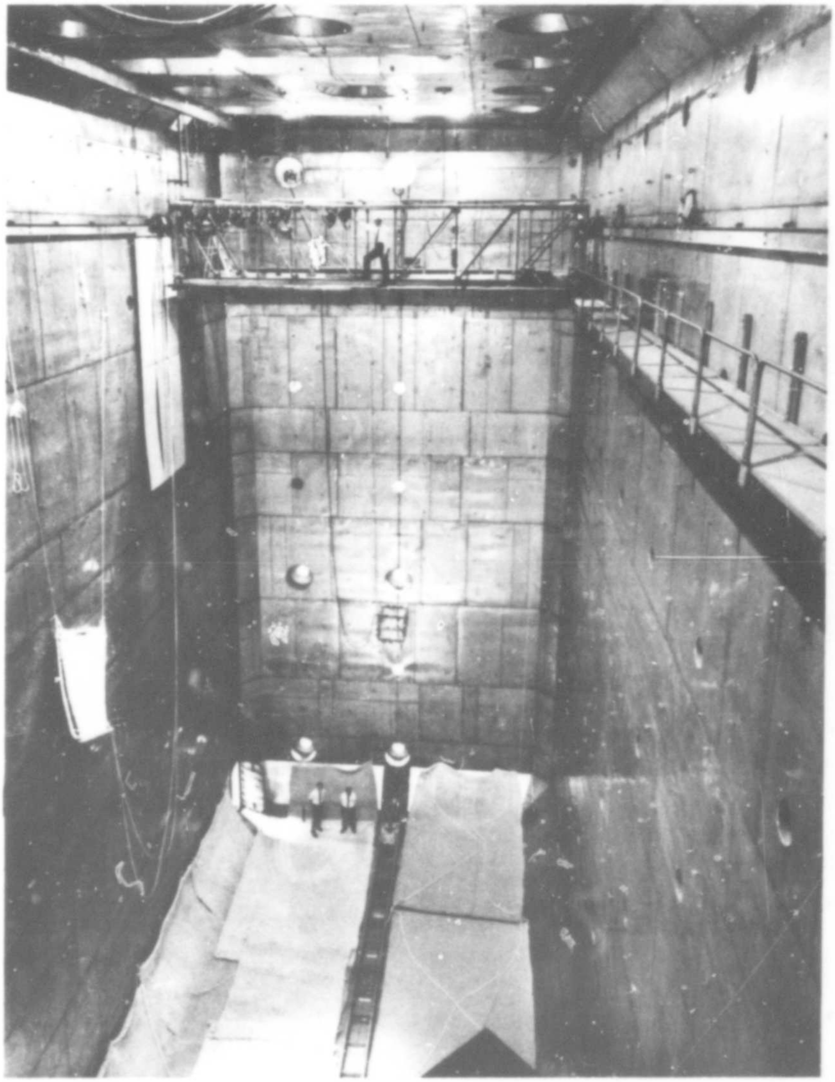

WATER TANK - 100 FEET LONG, 75 FEET DEEP, 35 FEET WIDE
WATER DEPTH - MAXIMUM OF 65 FEET
CONSTRUCTION - STAINLESS STEEL LINED TANK, SUPPORTED BY REINFORCED CONCRETE

FIG. 5 INTERIOR OF HYDRO BALLISTICS FACILITY

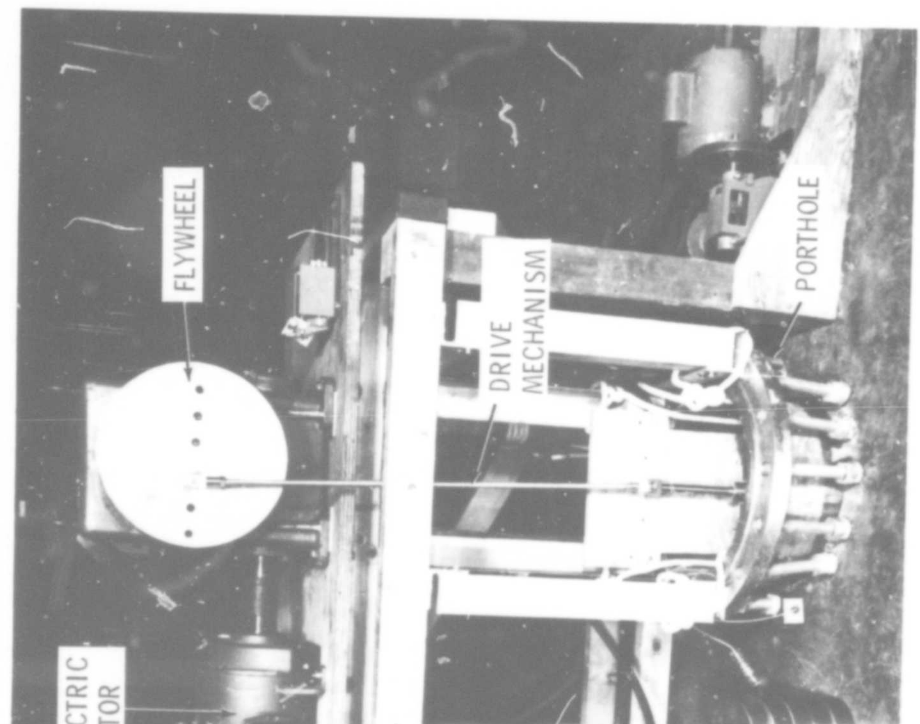

FIG. 6 TEST APPARATUS

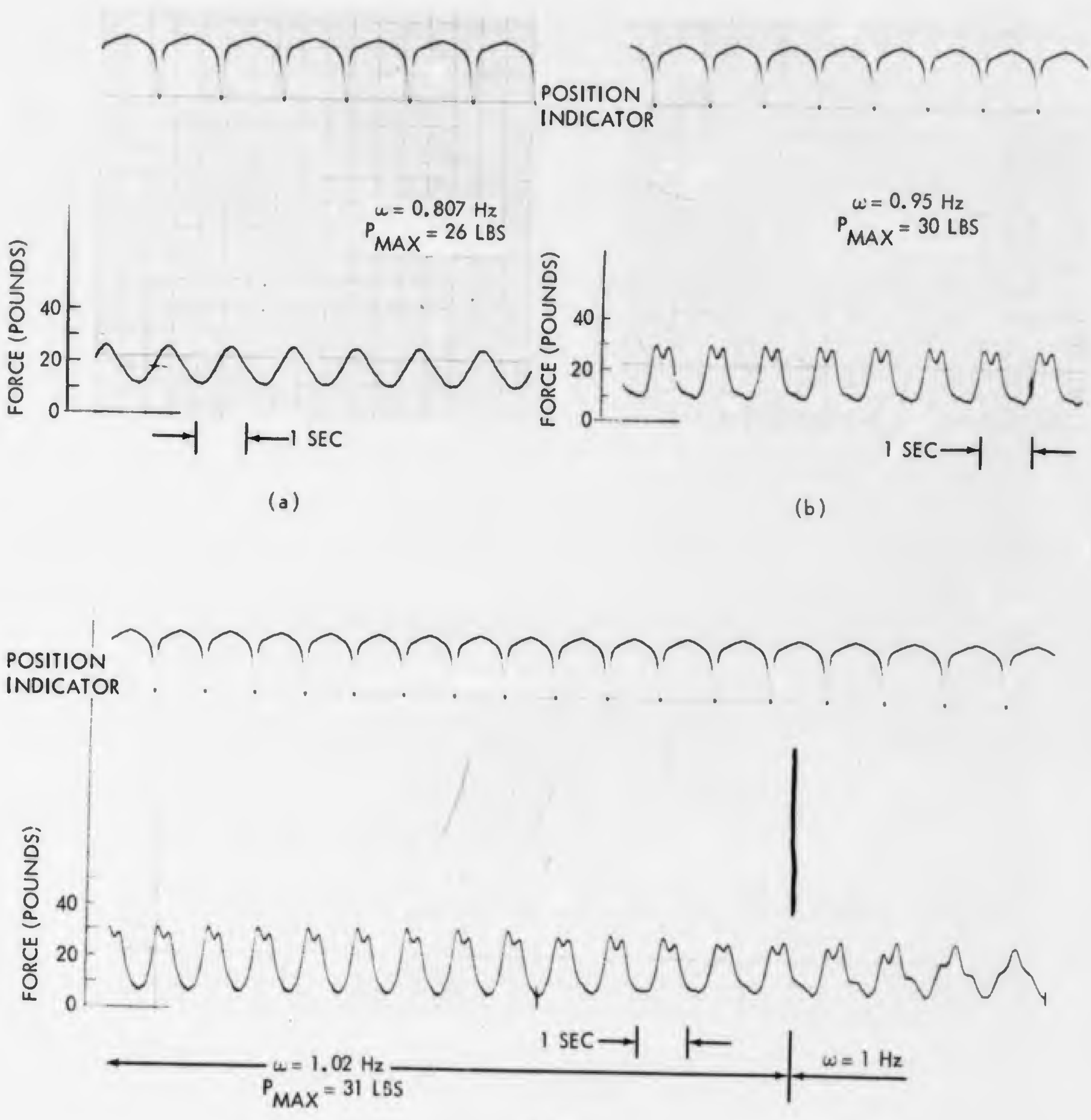

FIG. 7 EXPERIMENTAL FORCE RESPONSE AT TOP OF 1/16" STEEL CABLE IN WATER (SPECIMEN NO. 2) AT VARIOUS FORCING FREQUENCIES (X_o=3")

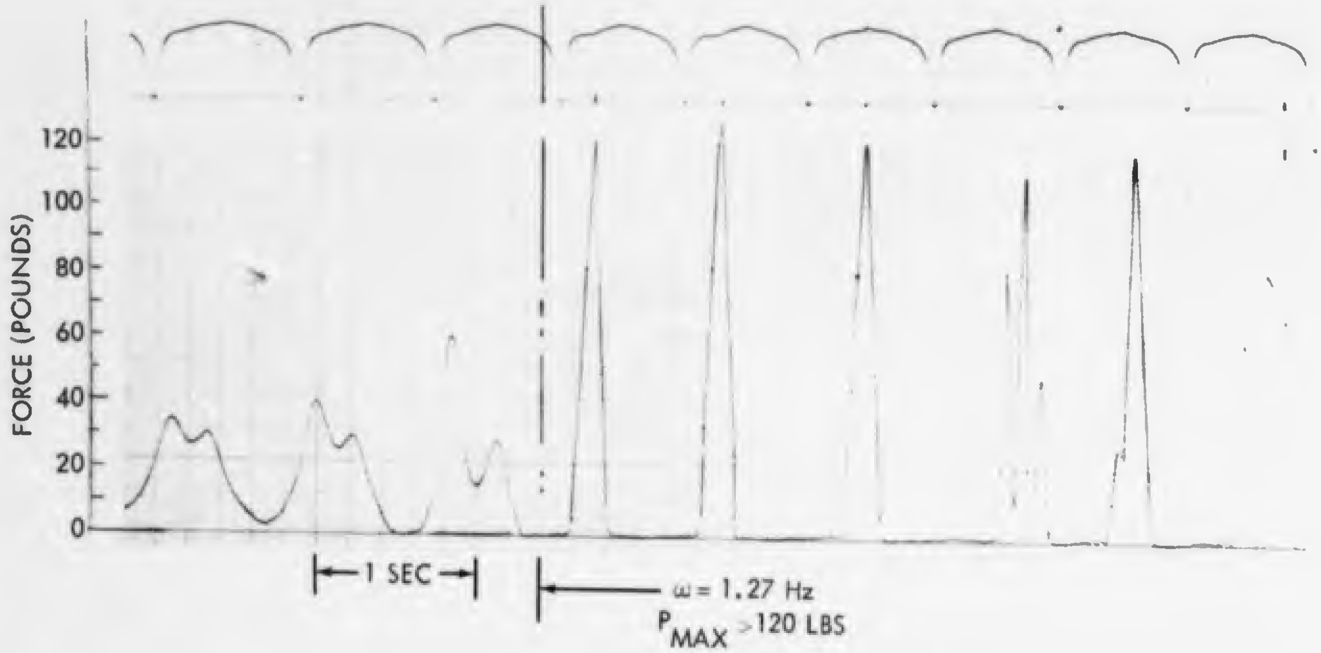

(d)

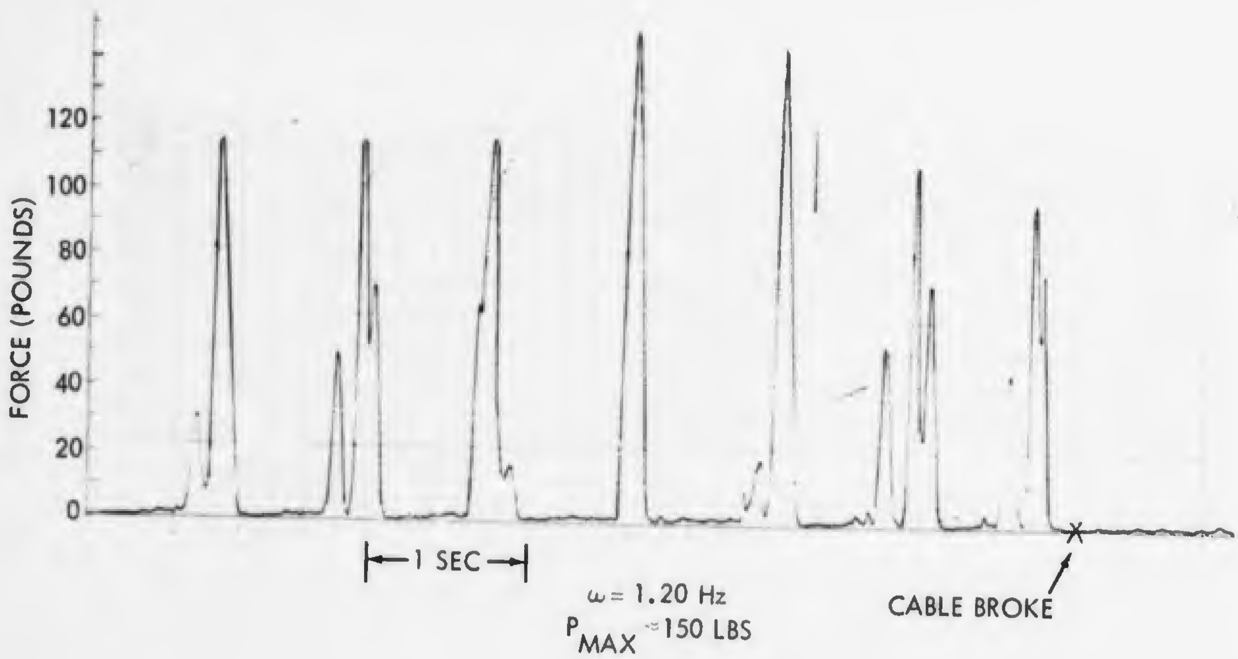

(e)

FIG. 7 CONTINUED

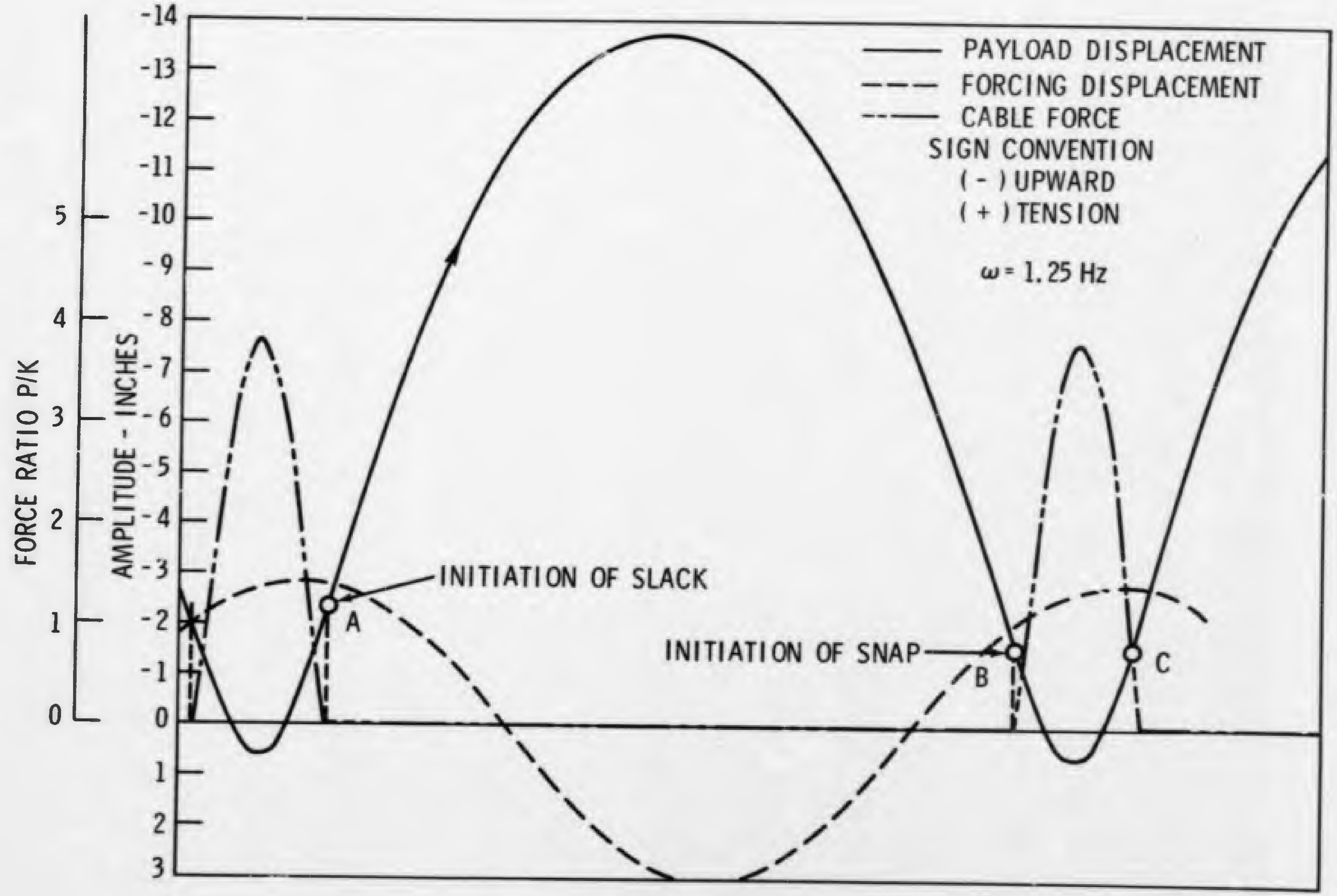

FIG. 8 DISPLACEMENT AND FORCE VERSUS TIME DURING SNAP OF 1/16" STEEL CABLE (SPECIMEN NO. 2)

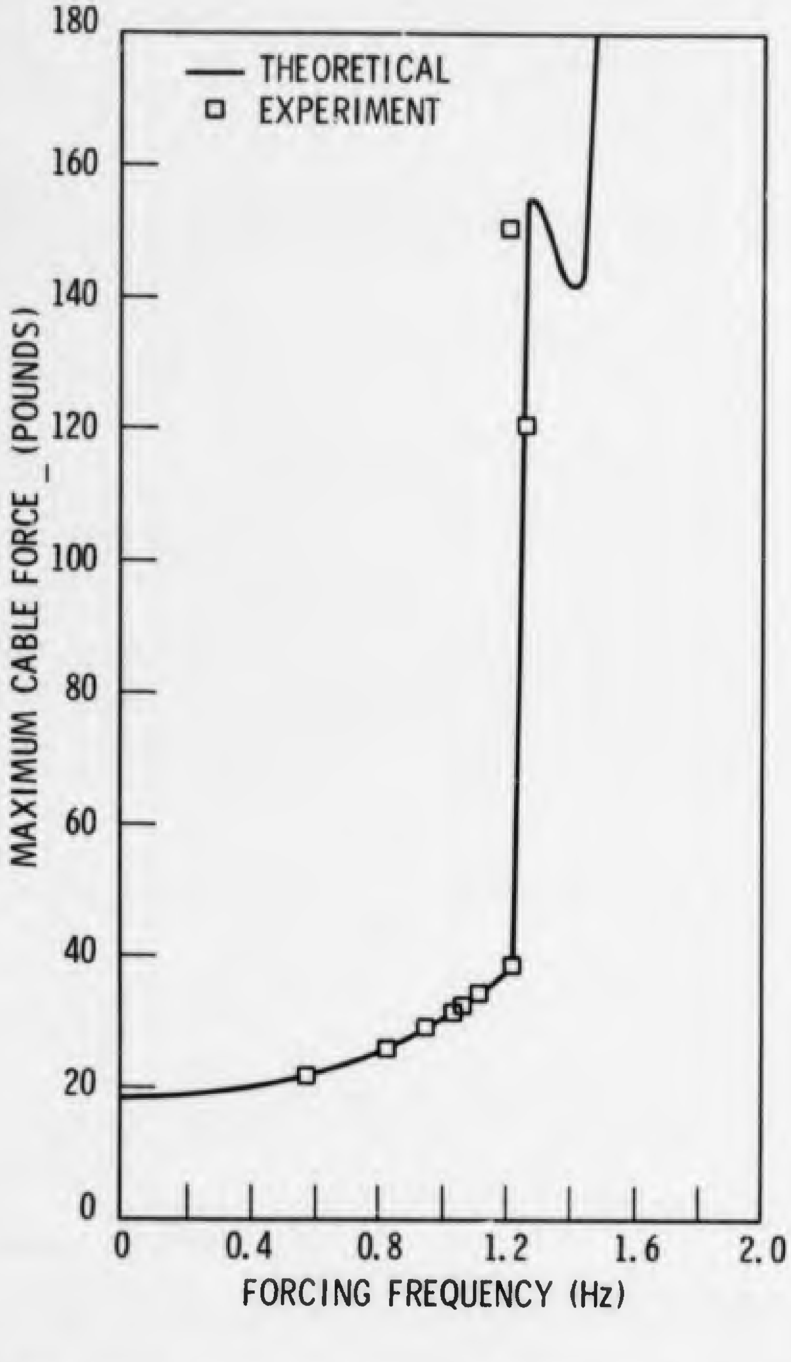

FIG. 9 FORCE AT TOP OF 1/16" STEEL CABLE (SPECIMEN NO. 2) VERSUS FORCING FREQUENCY - COMPARISON OF EXPERIMENT WITH DIGITAL PROGRAM (MODEL NO 2)

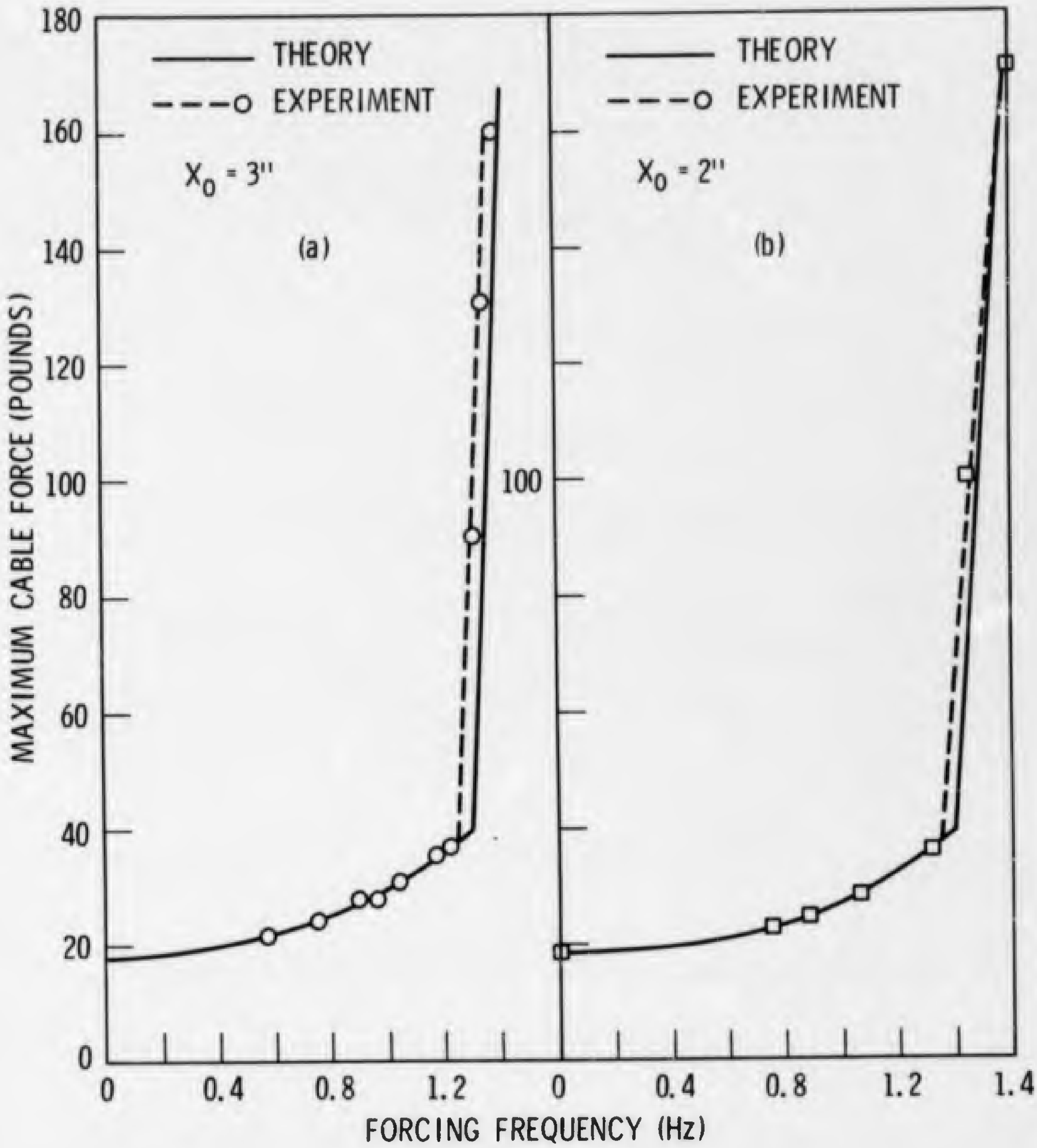

FIG. 10 FORCE AT TOP OF 3/32" STEEL CABLE (SPECIMEN NO. 1) VERSUS FORCING FREQUENCY - COMPARISON OF EXPERIMENT WITH DIGITAL PROGRAM (MODEL NO. 2)

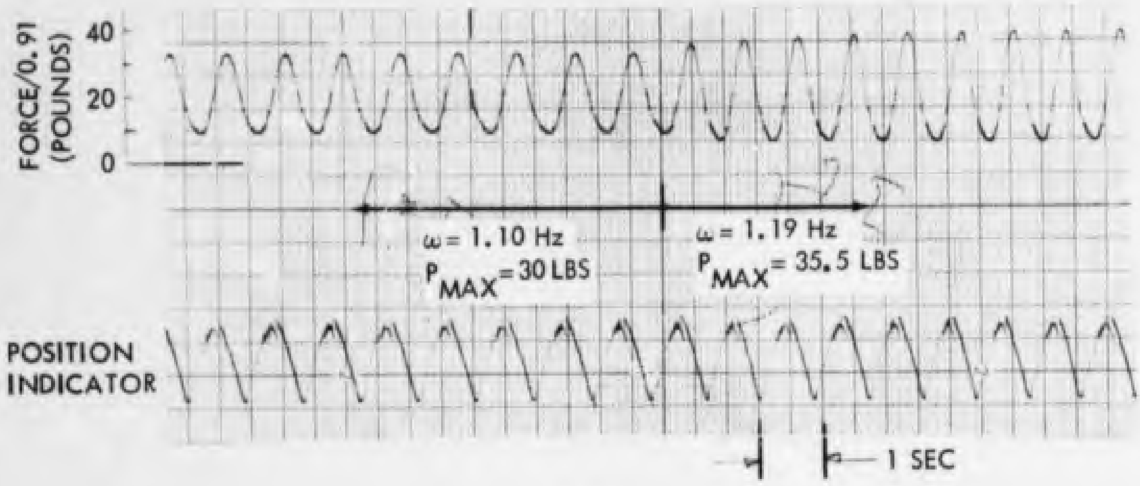

(a)

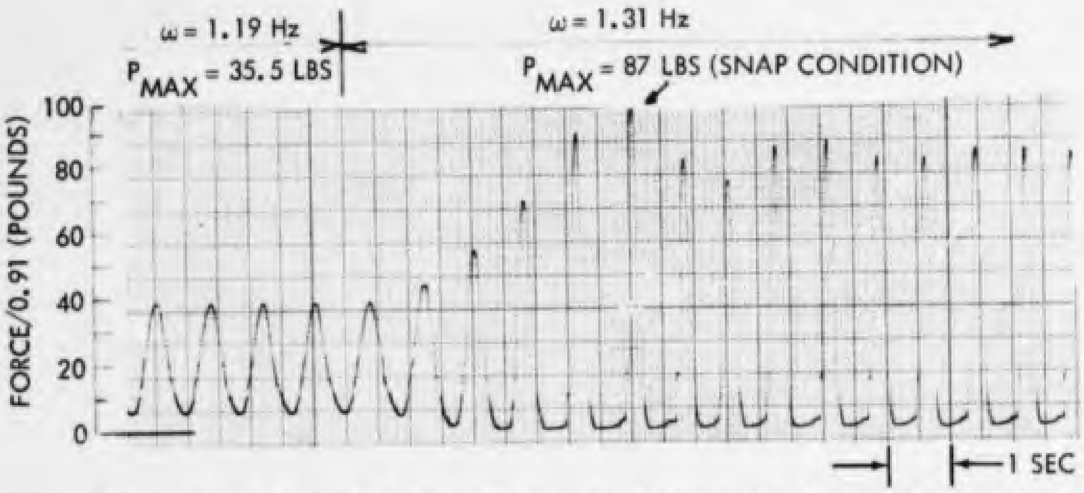

(b) FORCE RESPONSE GOING THROUGH RESONANCE - SNAP LOADING IS INITIATED

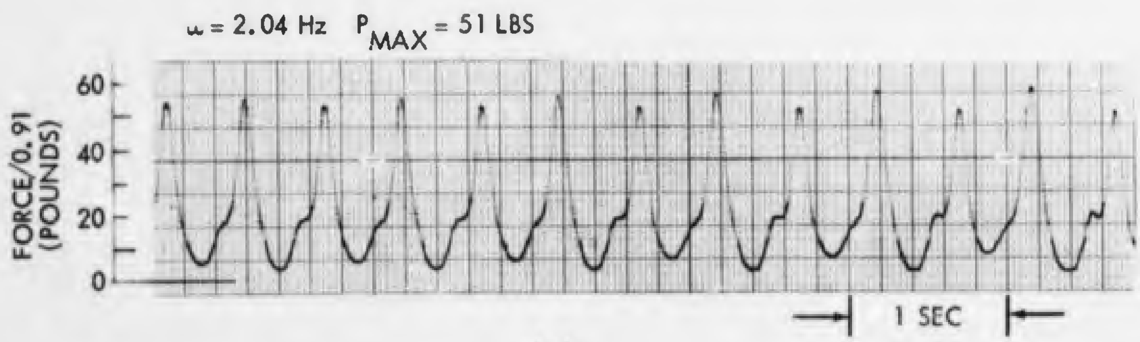

(c)

FIG. 11 EXPERIMENTAL FORCE RESPONSE AT TOP OF SPECIMEN NO. 5 IN WATER AT VARIOUS FREQUENCIES (X_o=2")

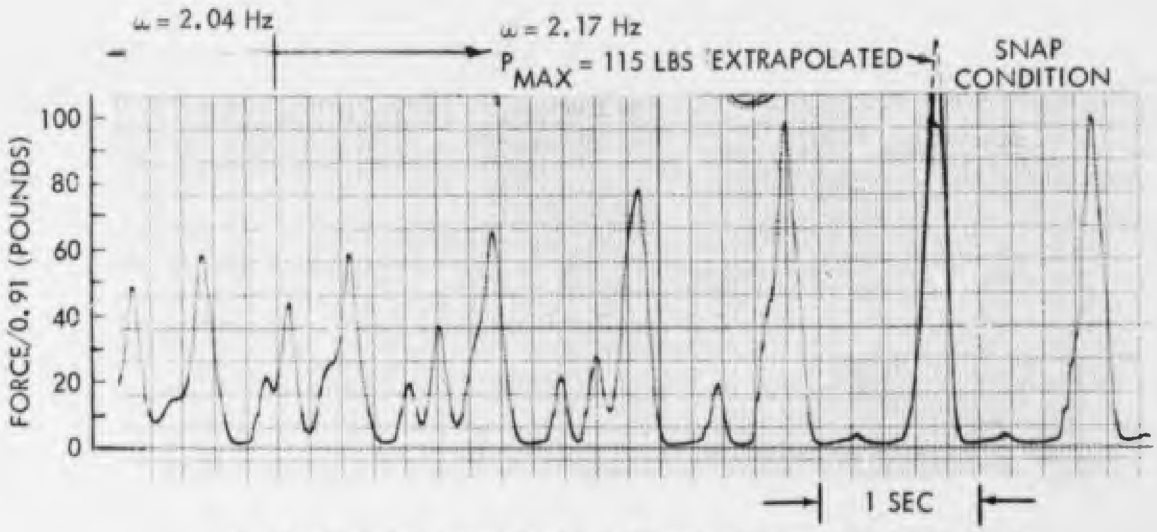

(d) FORCE GOING THROUGH SECOND RESONANCE CONDITION

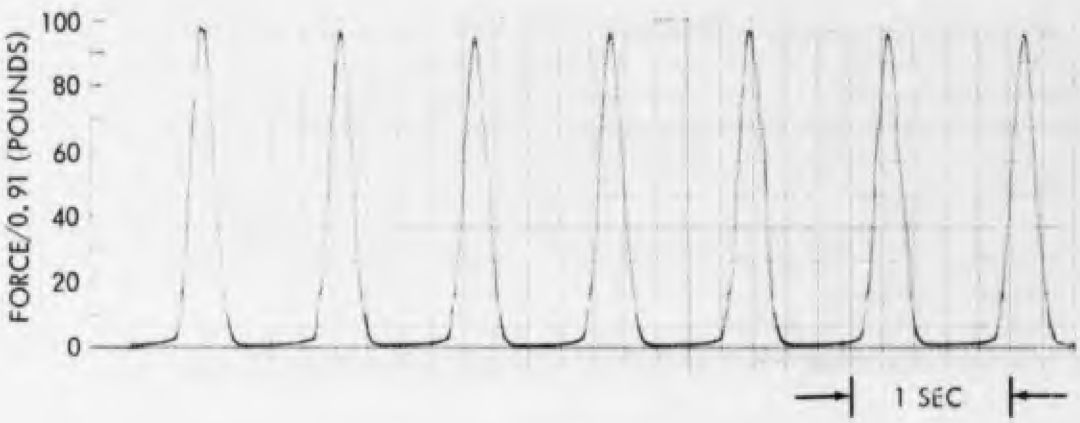

(e) SNAP CONDITION AFTER DECREASE OF FREQUENCY FROM MAXIMUM

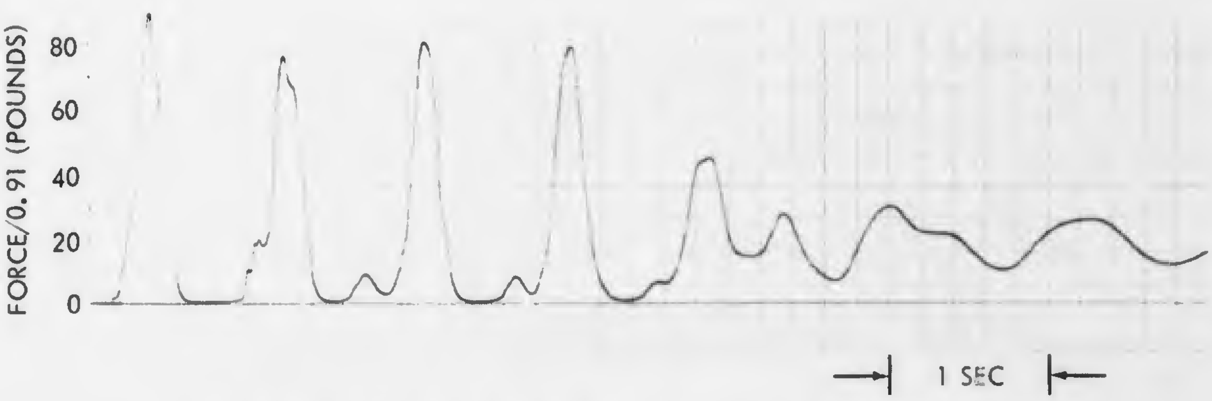

(f) RAPID DROPOFF IN FORCE WHILE REDUCING FORCING FREQUENCY FROM 1.17 HZ TO 0.91 HZ

FIG. 11 CONTINUED

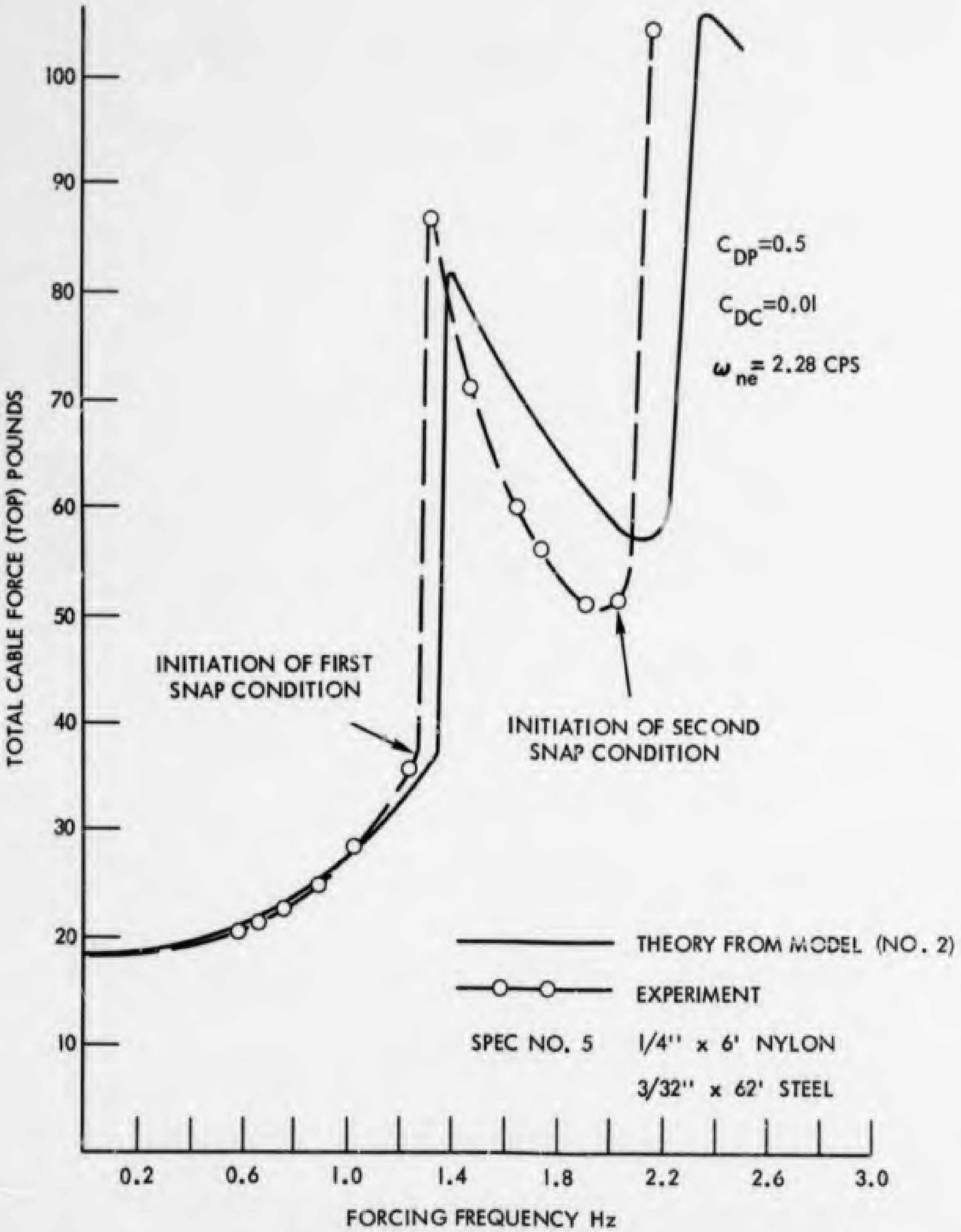

FIG. 12 MAXIMUM CABLE FORCE VERSUS FREQUENCY FOR SPECIMEN NO. 5 IN WATER SHOWING COMPARISON OF EXPERIMENT WITH MODEL (NO. 2) (X_0 2")

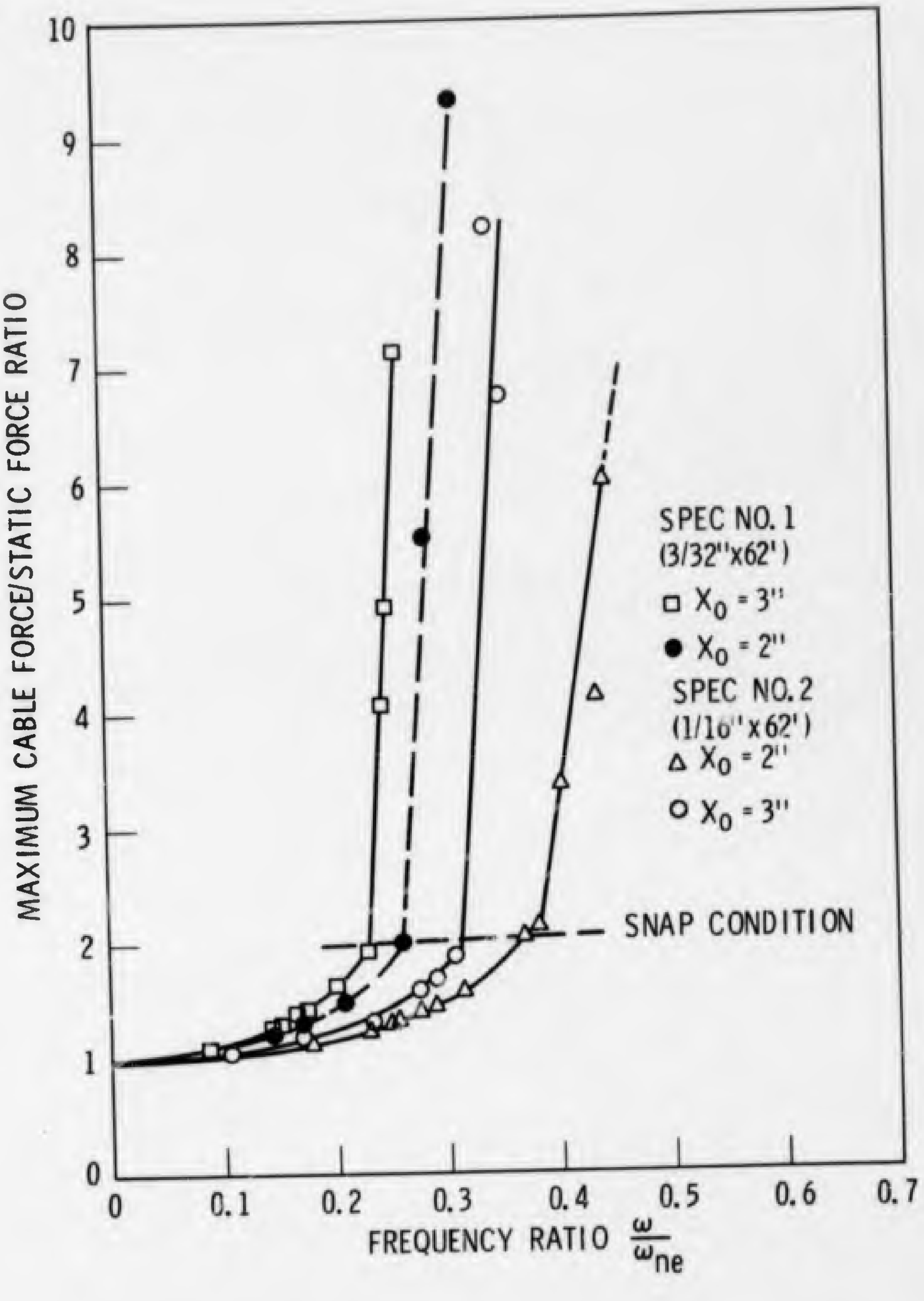

FIG. 13 EXPERIMENTAL FORCE RATIO P_{MAX}/T_{STAT} VERSUS FREQUENCY RATIO FOR 1/16" AND 3/32" STEEL CABLES

UNCLASSIFIED
Security Classification

DOCUMENT CONTROL DATA - R & D

(Security classification of title, body of abstract and indexing annotation must be entered when the overall report is classified)

1. ORIGINATING ACTIVITY (Corporate author) U. S. Naval Ordnance Laboratory White Oak, Silver Spring, Maryland 20910	2a. REPORT SECURITY CLASSIFICATION UNCLASSIFIED
	2b. GROUP

3. REPORT TITLE
A THEORETICAL AND EXPERIMENTAL INVESTIGATION OF SNAP LOADS IN STRANDED STEEL CABLES

4. DESCRIPTIVE NOTES (Type of report and inclusive dates)

5. AUTHOR(S) (First name, middle initial, last name)
Jack E. Goeller

6. REPORT DATE 26 November 1969	7a. TOTAL NO. OF PAGES 35	7b. NO. OF REFS 4
8a. CONTRACT OR GRANT NO.	9a. ORIGINATOR'S REPORT NUMBER(S) NOLTR 69-215	
b. PROJECT NO.		
c.	9b. OTHER REPORT NO(S) (Any other numbers that may be assigned this report)	
d.		

10. DISTRIBUTION STATEMENT
This document has been approved for public release and sale; its distribution is unlimited.

11. SUPPLEMENTARY NOTES	12. SPONSORING MILITARY ACTIVITY Naval Ordnance Systems Command

13. ABSTRACT
During longitudinal oscillation of a cable with a payload supported at the lower end, a severe impact load called snap can be experienced if the cable should go slack. This report presents an analog model and a digital program for computing snap loads in cables during longitudinal oscillation simulating ocean wave motion. The theory is shown to agree well with experimental tests on stranded steel cable oscillated in water. Schemes for mitigating the snap load are discussed.

DD FORM 1 NOV 65 1473 (PAGE 1)

S/N 0101-807-6801

UNCLASSIFIED
Security Classification